Journal of Materials Chemistry B

PAPER

View Article Online
View Journal | View Issue

Cite this: J. Mater. Chem. B, 2014, 2, 5461

Growth and accelerated differentiation of mesenchymal stem cells on graphene oxide/poly-L-lysine composite films†

Wei Qi,* Wenjing Yuan, Jing Yan and Hua Wang*

Received 27th May 2014
Accepted 24th June 2014

DOI: 10.1039/c4tb00856a

www.rsc.org/MaterialsB

A new type of composite films of graphene oxide (GO) and poly-L-lysine (PLL) have been fabricated for use as bio-scaffold coatings with improved mechanical properties. The morphology, growth and differentiation of mesenchymal stem cells (MSCs) on the GO/PLL composite films have been examined. The results demonstrated that the GO/PLL composite films could not only support the growth of MSCs with a high proliferation rate, but could accelerate the osteogenic differentiation of MSCs, showing strong alkaline phosphatase (ALP) and gene expression. Importantly, the high pre-concentration capacity of the GO/PLL films for osteogenic inducers could play a key role in accelerating the osteogenic differentiation of MSCs through the strong non-covalent binding and electrostatic interaction between them. Moreover, the mild and inexpensive fabrication strategy could be applicable to biomacromolecules including chitosan, gelatin, *etc.* Therefore, such a kind of composite film could provide a multifunctional and highly biocompatible scaffold coating tailored for potential application in stem cell research.

1 Introduction

Mesenchymal stem cells (MSCs) isolated from bone marrow have been shown to differentiate into a variety of cell lineages *in vitro*, including adipocytes, chondrocytes, myocytes and osteoblasts. The combination of MSCs with scaffold materials provides a promising strategy for cell therapy and tissue engineering.[1–4] Some natural biomaterials such as polypeptides have been investigated as potential scaffold materials for stem cell transplantation. For example, poly-L-lysine (PLL), with plentiful active amino groups and positive surface charges, is most commonly used in biomedical fields such as bioactive surfaces, drug delivery and or so for promoting cell adhesion and supporting cell growth.[5–7] However, mechanical properties of PLL are not good enough for some biomedical applications such as bone tissue engineering or bone regenerative medicine. Therefore, it is essential to develop nanocomposites based on PLL to improve its mechanical properties. Graphene and its derivative, graphene oxide (GO), is an attractive substance as a composite material, especially as polymer nanocomposites due to its extraordinary mechanical properties including high Young's modulus, hardness and excellent flexibility. Moreover, as reported previously, the incorporation of GO into a polymer multilayer could improve the film properties significantly.[8] On the other hand, biointerfaces composed of graphene or GO have been investigated for adhesion, proliferation and differentiation of the MSCs.[9–15] Particularly, GO, in which the basal plane and edges possess epoxide, carboxyl, and hydroxyl groups, enables greater interactions with biomacromolecules through covalent, electrostatic and hydrogen-bonding than graphene.

Herein, a new type of GO/PLL composite films have been built up in this study *via* layer-by-layer (LbL) assembly, for growth, proliferation and differentiation of stem cells (Fig. 1). The LbL assembly technique has been well recognized as a

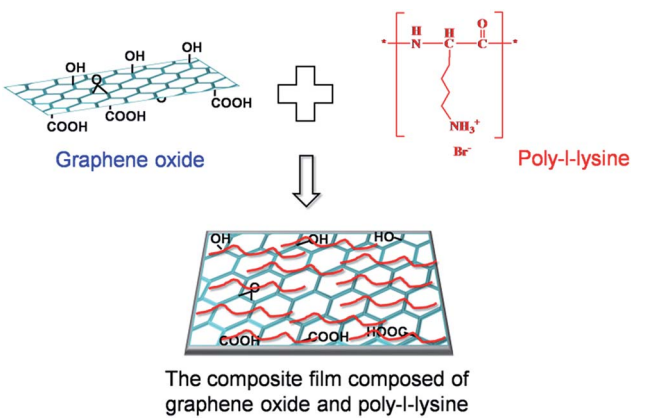

Fig. 1 Schematic representation of formation of the GO/PLL composite film.

Key Laboratory of Life-Organic Analysis, Key Laboratory of Pharmaceutical Intermediates and Analysis of Natural Medicine, School of Chemistry and Chemical Engineering, Qufu Normal University, 57 Jingxuan West Road, Qufu, Shandong 273165, China. E-mail: qf_qw@163.com; huawangqfnu@126.com; Tel: +86 537 4458208; +86 537 4456306

† Electronic supplementary information (ESI) available. See DOI: 10.1039/c4tb00856a

simple and versatile method to immobilize functional molecules.[16–23] Herein, the unique properties of GO, *i.e.* a large surface area and excellent mechanical properties, could be synergically coupled with the biocompatibility of PLL resulting in a kind of multifunctional scaffold coating, which can be used in tissue engineering and stem cell-based therapy.

2 Experimental

2.1 Materials

Expandable graphite (~180 μm) was obtained from Qingdao BCSM. CO., LTD. Poly-L-lysine (PLL) and phosphate buffer solution (PBS) were purchased from Sigma-Aldrich (USA). Calcein-AM and ethidium homodimer were obtained from Dojindo (Japan). Antibodies including anti-CD-44 and anti-osteocalcin (OCN) were purchased from Abcam (Hong Kong). Water used in this work was purified by a Milli-Q water system (Millipore, USA).

2.2 Fabrication and characterization of GO

Graphite oxide was obtained by the Hummers method.[8,24] Briefly, graphite oxide was obtained by oxidation of graphite with H_2SO_4, and $KMnO_4$. The formed graphite oxide was washed three times with 1.0 M of aqueous HCl solution and deionized water until a pH of 4.0–5.0 was achieved. During the washing process with deionized water, a graphene oxide gel formed. Following that, a freeze-dry procedure was conducted to obtain the graphene oxide solid. Atomic force microscopy (AFM, Digital Instruments, USA), UV-Vis spectroscopy (UV-1601, Shimadzu, Japan) and IR spectroscopy (NEXUS 470, Nicolet, USA) were used to characterize the GO nanosheets.

2.3 Preparation and characterization of the GO/PLL film

Glass coverslips (14 mm diameter or 4.5 mm diameter) were used as the substrates for LbL assembly. They were first cleaned in piranha solution (7 : 3 v/v H_2SO_4/H_2O_2) before use, followed by rinsing with water. PLL solutions were prepared at a concentration of 2 mg mL^{-1} in PBS, and GO dispersion was prepared at a concentration of 0.1 mg mL^{-1} in water. Then, PLL and GO were alternately assembled onto the cleaned glass slides. There were 15–20 minutes for each deposited layer and three rinses in water until 4 cycles. The obtained $(GO/PLL)_4$ film was also characterized using AFM, UV-Vis spectroscopy and IR spectroscopy.

2.4 Cell culture

Rat bone marrow derived MSCs were obtained from commercial sources (Tianjin Weikai Bioeng Ltd., China) and were cultured in low-glucose DMEM medium (Gibco, USA), supplemented with 10% fetal bovine serum (Invitrogen, USA), 1% penicillin/streptomycin (Invitrogen, USA). Herein, the MSCs at passage 4 were used.[25,26] The MSCs (2×10^4 cells per well, 24-well plate) were seeded on all the surfaces separately and cultured under the same conditions. All the studied surfaces were sterilized in advance and placed within a cell culture polystyrene well. For cell viability, live/dead staining with calcein-AM (to stain live cells with green color) and ethidium homodimer (to stain dead cells with red color) was employed. For the purpose of comparison, cell counting kit-8 (CCK-8) assays (Dojindo, Japan) were carried out for all the studied cells. The morphology of the MSCs on all the surfaces was observed by using a phase contrast microscope (Olympus CKX31, Japan). The population doubling times (PDT) of cells on all the studied surfaces were determined with the growth kinetics and the following equation.[27]

$$\mathrm{PDT} = (t_2 - t_1)\frac{\lg 2}{\lg N_2 - \lg N_1} \quad (1)$$

N_2: number of cells at time t_2, and N_1: number of cells at time t_1.

2.5 Osteogenic differentiation

For osteogenic differentiation, the MSCs cultured on all the surfaces for 1 day were transferred to the osteogenic medium (Tianjin Weikai Bioeng Ltd., China) consisting of DMEM basal medium added with dexamethasone (10^{-8} M), β-glycerol phosphate (10 mM), and ascorbic acid (0.2 mM). The medium was changed every 3 days until confluence.[25,26] Alkaline phosphatase (ALP) staining was performed using BCIP/NBT stock solution (Beyotime, China) and ALP quantification was done using an alkaline phosphatase assay kit (Abcam, Hong Kong) at day 2, 7, 12, and 15.

2.6 Immunofluorescence staining

First, the cells on all the surfaces were fixed with 3.7% formaldehyde solution over 30 min separately. After washing with PBS three times, the cells were incubated in 0.2% Triton X-100 for 10 min. Then, the cells were treated with 10% fetal bovine serum in PBS for 30 min. After removing the blocking agent, the antibodies to cellular markers (CD-44 for MSCs and OCN for osteoblasts) were added onto the separate substrates. After being incubated for 1 h, the substrates were exclusively washed with PBS and further were incubated with the diluted secondary antibody (Dyelight 488 goat anti-mouse antibody) for 30 min in the dark. Subsequently, the cells were stained by DAPI (Sigma-Aldrich, USA) for 30 min to color the nuclei. Finally, in all the cases, the cells were analyzed by using a confocal fluorescence microscope using the Olympus system and its software package (Olympus FV 1000, Japan).

2.7 Statistical analysis

Fluorescent microscopy images were evaluated and analyzed using ImageJ software (NIH, USA). Statistical analysis was performed using SPSS 13.0 to evaluate at least 10 images to determine statistical differences ($* < 0.05$) among all samples or between samples and controls, respectively. All experiments were repeated at least three times in triplicate and all values were presented as mean ± SD.

2.8 Adsorption of the chemical inducers

Dexamethasone, β-glycerol phosphate, and ascorbic acid were prepared separately in PBS with the concentration of 1 mM, 2 mM, 3 mM, 6 mM, and 10 mM, respectively. The solutions

with the concentration of 10 mM were employed for adsorption kinetics with the addition of the substrates. The adsorption of the chemicals was evaluated with UV-Vis spectroscopy. The amount of the adsorbed was determined from the change in absorption before and after the adsorption.

3 Results and discussion

3.1 Fabrication and characterization of GO and GO/PLL film

GO can be obtained by chemical oxidation and exfoliation of graphite. The produced GO was confirmed first by the atomic force microscopy (AFM) technique. It was found that the GO sheets had lateral dimensions of one to several hundred nanometers with a thickness of 1.0 nm approximately (Fig. S1†), which is characteristic of the fully exfoliated GO sheets.[28] Then the FTIR spectrum was used to characterize the produced GO. In Fig. S2,† the GO spectrum showed the presence of O–H (3430 cm^{-1}), C=O (1733 cm^{-1}), C=C (1630 cm^{-1}), and C–O (1128 cm^{-1}).[29] As a contrast, besides these sites, the IR spectrum of the LbL-assembled $(GO/PLL)_4$ composite film exhibited PLL absorption features, such as N–H (3259 cm^{-1}), C=O (1633 cm^{-1}) and C–N (1552 cm^{-1}). Also, the nanotopography and thickness of the $(GO/PLL)_4$ film were determined by AFM. Fig. 2A shows clearly the existence of GO sheets on the film surface showing the thickness of the $(GO/PLL)_4$ film of 5.51 nm (Fig. S3†). The buildup of the GO/PLL films was further monitored by UV-Vis spectroscopy (Fig. 2B). Comparing with the UV-Vis spectrum of PLL, all the spectra of the GO/PLL films manifested the absorption peaks at 240 nm, and 310 nm. They are characteristic absorption of GO from the π–π* transitions of aromatic C–C bonds and n–π* transitions of C=O bonds, respectively. These results confirmed the successful formation of the GO/PLL composite film.

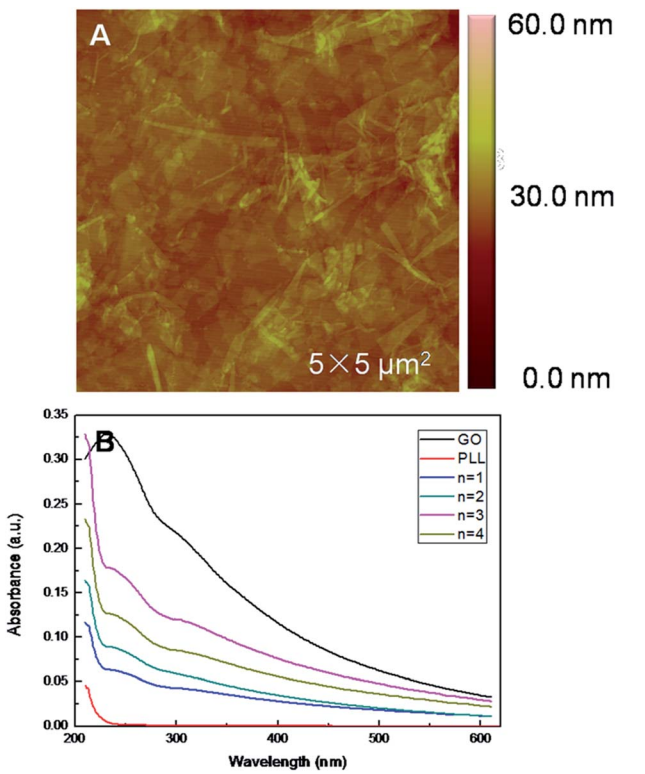

Fig. 2 (A) AFM image of the $(GO/PLL)_4$ film; (B) UV-Vis absorption spectra of GO, PLL and the $(GO/PLL)_n$ film, $n = 1, 2, 3, 4$.

3.2 MSCs viability and proliferation on the GO/PLL film

To determine whether or not the GO/PLL film had a significant effect on the MSCs, fluorescence staining was performed using calcein-AM (to stain live cells with green color) and ethidium homodimer (to stain dead cells with red color). Fluorescence microscopy revealed that most of the MSCs plated on the composite films were alive, as shown in Fig. 3A. From the phase contrast image (Fig. 3B), the cells displayed the polygonal and flattened cell morphology on the GO/PLL film and presented the elongated structure with their spindle shape. The morphology of cells on the other studied surfaces is shown in Fig. S4.† Additionally, a cell count kit-8 (CCK-8) assay was carried out to confirm the cell viability data after 1 day and 7 day of cell culture on the composite film respectively. Glass coverslips (treated with piranha solution), GO-coated coverslips (GO-coverslips) fabricated with the spin coating technique, PLL coated glass coverslips (PLL-coverslips) and tissue culture polystyrene (TCPS) were employed for comparison. As shown in Fig. 3C,

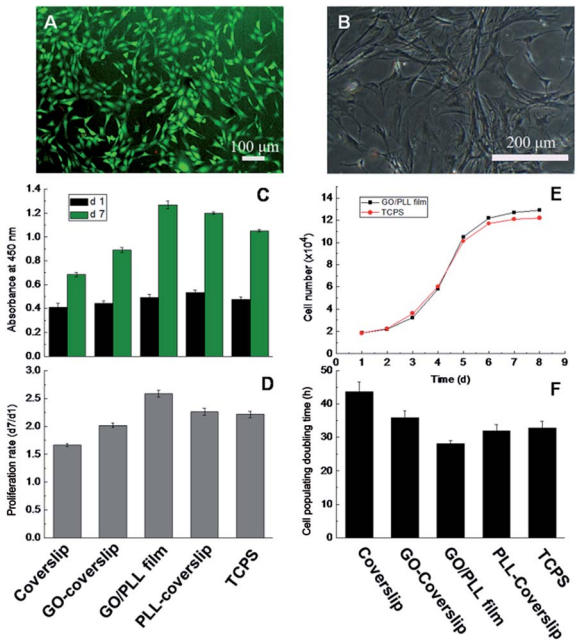

Fig. 3 (A) Fluorescence images of MSCs were obtained on the $(GO/PLL)_4$ film by live/dead staining of cells after incubation for 3 days. Live cells were stained fluorescence green, and dead cells appeared red. (B) Phase contrast images of MSCs cultured for 3 days on the $(GO/PLL)_4$ film in normal cell culture media. (C) Cell viabilities of MSCs cultured on all the studied surfaces in cell culture media by day 1 and day 7. (D) Cell proliferation on all the studied surfaces as estimated by the ratio (D7/D1). (E) Growth kinetics of cells on the TCPS and GO/PLL composite films. (F) The population doubling times of cells on all the studied surfaces. The total number of cells was determined at different time points to obtain the doubling time.

almost no difference was noted in the cell viability on all the studied surfaces after being cultured for 1 day (D1). While on the 7th day of culture, the cell viability of MSCs on the composite film was 186.0%, 142.7%, 105.8% and 120.7% greater than those on the glass coverslips, GO-coverslips, PLL-coverslips, and TCPS (D7), respectively. Cell proliferation was estimated by the ratio of absorbance value D7/D1 and the values were shown in Fig. 3D. It could be seen that the proliferation of cells on the PLL-coverslips was nearly equal to those on TCPS, and that of the GO-coverslips was about 20% lower. While significant proliferation was observed for the $(GO/PLL)_4$ film. The high proliferation may be attributed to the synergistic coupling effects of GO and PLL, which will be investigated further in this work. In Fig. 3E, growth kinetics of cells on the TCPS and the GO/PLL film was recorded. Accordingly, the population doubling time was analyzed at multiple time points over the culture period. In comparison, the doubling time of cells on the composite film was 28.07 h, and decreased from those on TCPS (32.82 h) (Fig. 3F). These results suggested that the GO/PLL film did not hamper the normal growth of stem cells but rather provided a suitable environment for the proliferation of MSCs.

3.3 Osteogenic differentiation of MSCs on the GO/PLL film

Then, when cultured in osteogenic media, the MSCs were determined and analyzed osteogenesis using alkaline phosphatase (ALP) staining as a marker.[30] On the 2nd day of differentiation, cells cultured on all the substrates showed no difference in ALP production. There was negative staining and absolutely no ALP production was observed from the images shown in Fig. 4A. By day 7, cells on the film were stained positively and the cytoplasm was stained blue-black. ALP staining results of MSCs on the 7th day of differentiation on the other studied surfaces are shown in Fig. S5.† Also, quantitative ALP staining was used to study the differentiation of MSCs on all the studied substrates (Fig. 4B). The cells on the GO-coverslips and the PLL-coverslips expressed ALP obviously from day 7, and the ALP activity increase gradually till day 15. The ALP activity of cells on the PLL-coverslips was a little higher than that of GO-coverslips and TCPS, respectively. Again, significant ALP production by cells were seen on the $(GO/PLL)_4$ film by day 7. Importantly, from day 7 onward, the cells grown on the film showed higher ALP activity than those on the surfaces as controls obviously. And, the activity of cells on the GO/PLL film on the 12th day of differentiation was nearly equal to that of 15th day. Therefore, the GO/PLL film supported and accelerated the osteogenic differentiation of MSCs showing the apparent osteogenesis during the osteogenic differentiation process.

Furthermore, osteocalcin (OCN) as one of the osteogenic genes was examined to confirm the osteogenic differentiation of MSCs on the $(GO/PLL)_4$ film. Since CD-44 is one of the characteristic genes for stem cells, its expression was also checked for the MSCs cultured on the samples.[15] Herein, the protein expression was compared by the intensity of fluorescence *via* immunofluorescence staining, where the cells were stained with DAPI (blue), CD-44 and OCN (green). As verified in Fig. 5A, the CD-44 could be visible clearly still by day 2, however, the intensity of fluorescence decreased significantly by day 7 and completely disappeared by day 12. On the other hand, a progressive enhancement of fluorescence was observed by the OCN recognition from day 7 to day 12 (Fig. 5B). The protein expression of cells on the TCPS and blank glass coverslips were shown as comparison in Fig. S6 and S7,† respectively.

Also, the differentiation of MSCs on all the studied surfaces was compared by the ratio of CD-44 (Fig. 6A), OCN (Fig. 6B) positive cells in all the cells by day 2, 7, 12, respectively. As demonstrated in Fig. 6B, cell differentiation was accelerated on

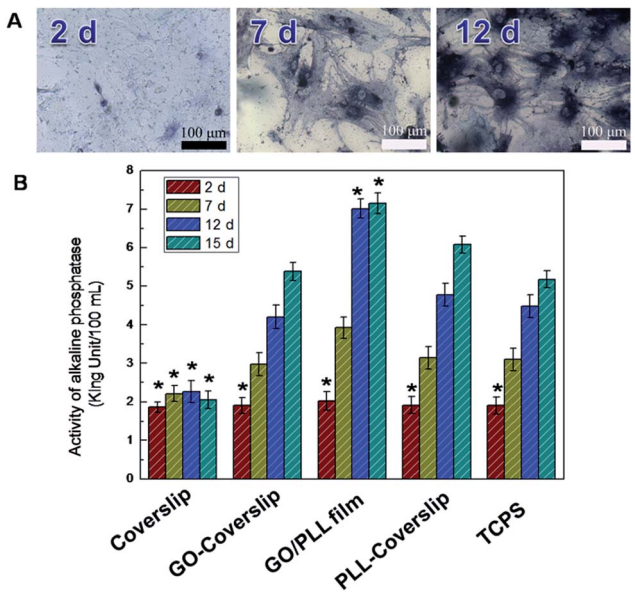

Fig. 4 (A) ALP staining results of MSCs on the $(GO/PLL)_4$ film for 2, 7, and 12 days, respectively. The scale bar is 100 μm. (B) Activity of ALP produced from cells cultured for 2, 7, 12, and 15 days on all the studied surfaces.

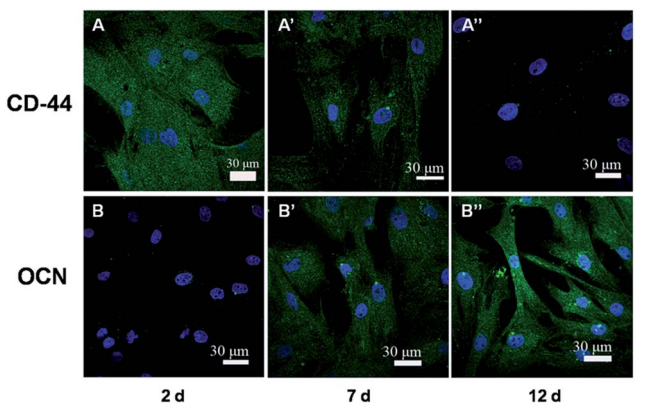

Fig. 5 Immunostaining of cells growing on the $(GO/PLL)_4$ film was performed from 2 days to 12 days. Cells are stained with DAPI (blue) and CD-44 or osteocalcin (OCN) as indicated (green). (A, A′ and A″) CD-44, marker for stem cells, decreased over time and completely disappeared by day 12. (B, B′ and B″) OCN, marker for osteoblasts, became visible at day 7 and very intense by day 12.

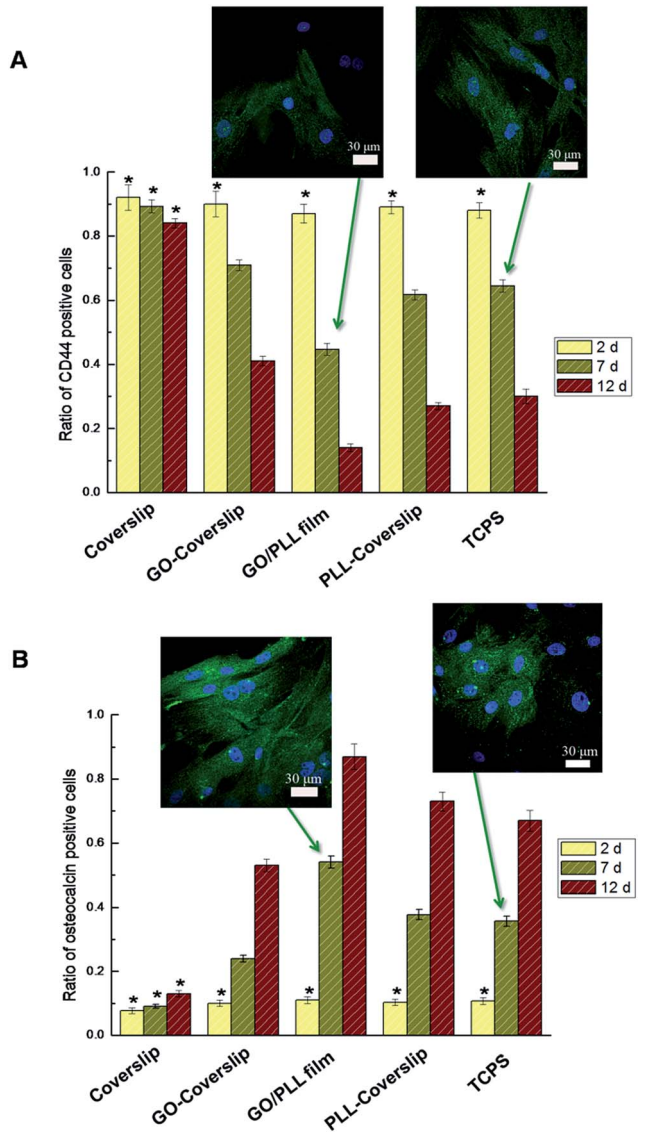

Fig. 6 Immunofluorescent (A) CD-44 and (B) OCN staining of MSCs grown on the $(GO/PLL)_4$ film (left) and on the TCPS (right). The histogram is the ratio of positively stained cells and the sum of positively and negatively stained cells on all the studied substrates by day 2, 7, and 12, respectively.

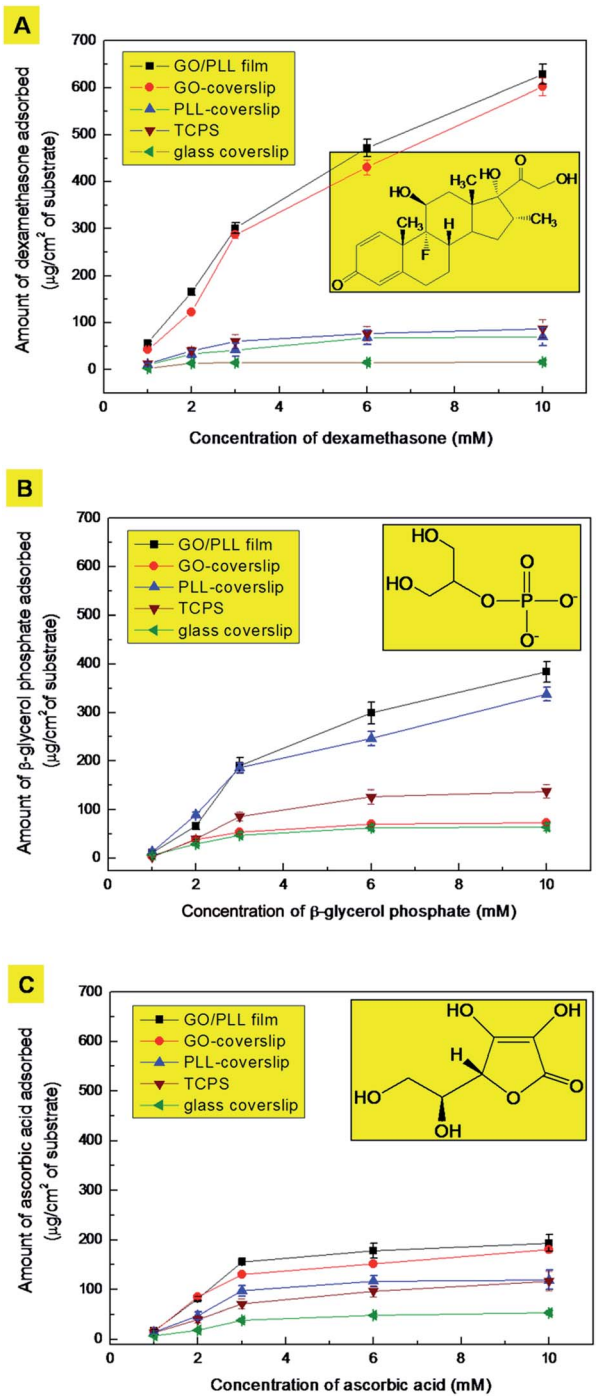

Fig. 7 Loading capacity of (A) dexamethasone, (B) β-glycerol phosphate, (C) ascorbic acid in different concentration on all the studied surfaces. The insets are the chemical structures, respectively.

the GO/PLL film by day 7, as compared to those on TCPS, showing nearly 55% positive OCN while the latter showed 35% positive. Taken together, these results indicated that the GO/PLL film could promote the osteogenesis of MSCs significantly. Herein, the predominance of the GO/PLL composite films over the GO surface and the PLL surface might be the results of coupled combination of two components, which could be evidenced by the following study.

Since the conventional osteogenic media can directly mediate the differentiation, a direct correlation with the adsorption of the substrate for the osteogenic chemical inducers was thought to be involved.[15,31] And what is more, previous studies have recognized that GO has the remarkable loading capacities for proteins, DNA and or so, *via* its large surface area and intermolecular interaction.[32–34] Therefore, the adsorption of the $(GO/PLL)_4$ film for the chemical inducers was investigated using UV spectrophotometry. First, the loading capacities of the film for the osteogenic chemicals, dexamethasone, β-glycerol phosphate, ascorbic acid, were determined with the adsorption kinetics recorded in Fig. S8.† Furthermore, the adsorption of the chemicals on the studied substrates was also determined with increasing concentration of the

adsorbents (Fig. 7). The adsorbed amount was expressed in μg cm^{-2} of substrates. It was found that the $(GO/PLL)_4$ film could largely adsorb dexamethasone (10 mM), glycerol phosphate (10 mM), ascorbic acid (10 mM), with the loading amount of 629, 384 and 194 μg cm^{-2} of substrate by day 3, respectively. The high adsorption capacity of the GO/PLL film and the GO-coverslip for dexamethasone may be attributed to the π–π stacking between the aromatic rings in the organic molecules and the graphene basal plane. As for the adsorption of β-glycerol phosphate, the electrostatic attraction between the anions and the positively charged PLL molecules from the GO/PLL film as well as the PLL-coverslip could play a major role during the adsorption process. While in the case of ascorbic acid, the hydrogen-bond between ascorbic acid and GO should be considered to push the adsorption of ascorbic acid into the GO/PLL film and the GO-coverslips. Therefore, it may be deduced that the high adsorption capacity of the GO/PLL film for these chemical inducers could cause the inducers to be locally concentrated on the film to facilitate cell–substrate interactions resulting in great enhancement of osteogenic differentiation of MSCs.

4 Conclusions

In summary, a new type of GO/PLL composite films has been fabricated *via* LbL assembly in a mild and inexpensive way, which could be applicable to other kinds of biomacromolecules such as chitosan, gelatin, *etc.* It has been demonstrated that the GO/PLL composite film could enhance the differentiation of MSCs to the osteoblast lineage without influencing the shape and the growth of MSCs. Moreover, compared to the commercial materials such as TCPS or glass coverslips, the GO/PLL film could obviously preconcentrate the osteogenic inducers, *i.e.* dexamethasone, β-glycerol phosphate and ascorbic acid. It might play a key role in the significant enhancement of osteogenic differentiation of MSCs on the composite film. Overall, the GO/PLL film as well as the film fabrication strategy could be promising for clinical applications in tissue engineering or regenerative medicine with easy fabrication, biocompatibility, and versatility.

Acknowledgements

W. Q. thanks Dr Qingmin Ji and Dr Katsuhiko Ariga, International Center for Materials Nanoarchitectonics (MANA), National Institute for Materials Science (NIMS), for their technical supports and valuable discussions. This work was financially supported by the National Nature Science Foundation of China (no. 21003084, 21375075), the Student Research Training Program of Qufu Normal University (no. 2013A046), and the Taishan Scholar Foundation of Shandong Province, China.

Notes and references

1 Q. Zhang, H. Lu, N. Kawazoe and G. Chen, *Acta Biomater.*, 2014, **10**, 2005.
2 H. Lu, N. Kawazoe, T. Kitajima, Y. Myoken, M. Tomita, A. Umezawa, G. Chen and Y. Ito, *Biomaterials*, 2012, **33**, 6140.
3 M. F. Pittenger, A. M. Mackay, S. C. Beck, R. K. Jaiswal, R. Douglas, J. D. Mosca, M. A. Moorman and D. W. Simonetti, *Science*, 1999, **284**, 143.
4 X. Wang, W. Song, N. Kawazoe and G. Chen, *J. Biomed. Mater. Res., Part A*, 2013, **101**, 3388.
5 J. Zhu, Y. Zhang, N. Xu, L. Wang, X. Xiang and X. Zhu, *J. Biomater. Sci., Polym. Ed.*, 2013, **24**, 1721.
6 C. Zheng, M. Zheng, P. Gong, J. Deng, H. Yi, P. Zhang, Y. Zhang, P. Liu, Y. Ma and L. Cai, *Biomaterials*, 2013, **34**, 3431.
7 Y. Liu and L. Yobas, *Biosens. Bioelectron.*, 2013, **50**, 78.
8 W. Qi, Z. Xue, W. Yuan and H. Wang, *J. Mater. Chem. B*, 2014, **2**, 325.
9 A. Higuchi, Q.-D. Ling, Y. Chang, S.-T. Hsu and A. Umezawa, *Chem. Rev.*, 2013, **113**, 3297.
10 A. F. de Faria, D. S. T. Martinez, S. M. M. Meira, A. C. M. de Moraes, A. Brandelli, A. G. S. Filho and O. L. Alves, *Colloids Surf., B*, 2014, **113**, 115.
11 C. Chung, Y.-K. Kim, D. Shin, S.-R. Ryoo, B. H. Hong and D.-H. Min, *Acc. Chem. Res.*, 2012, **46**, 2211.
12 J. Kim, Y.-R. Kim, Y. Kim, K. T. Lim, H. Seonwoo, S. Park, S.-P. Cho, B. H. Hong, P.-H. Choung, T. D. Chung, Y.-H. Choung and J. H. Chung, *J. Mater. Chem. B*, 2013, **1**, 933.
13 T. R. Nayak, H. Andersen, V. S. Makam, C. Khaw, S. Bae, X. Xu, P.-L. R. Ee, J.-H. Ahn, B. H. Hong, G. Pastorin and B. Özyilmaz, *ACS Nano*, 2011, **5**, 4670.
14 H. Zhang, G. Grüner and Y. Zhao, *J. Mater. Chem. B*, 2013, **1**, 2542.
15 W. C. Lee, C. H. Y. X. Lim, H. Shi, L. A. L. Tang, Y. Wang, C. T. Lim and K. P. Loh, *ACS Nano*, 2011, **5**, 7334.
16 G. Decher, *Science*, 1997, **277**, 1232.
17 N. J. Shah, J. Hong, Md. N. Hyder and P. T. Hammond, *Adv. Mater.*, 2012, **24**, 1445.
18 K. Ariga, Q. M. Ji, T. Mori, M. Naito, Y. Yamauchi, H. Abec and J. P. Hill, *Chem. Soc. Rev.*, 2013, **42**, 6322.
19 K. Ariga, Q. Ji, J. P. Hill, Y. Bando and M. Aono, *NPG Asia Mater.*, 2012, **4**, e17, DOI: 10.1038/am.2012.30.
20 J. Pennakalathil and J.-D. Hong, *ACS Nano*, 2011, **5**, 9232.
21 A. K. Sarker and J.-D. Hong, *Langmuir*, 2012, **28**, 12637.
22 W. Cui, Y. Cui, J. Zhao and J. Li, *J. Mater. Chem. B*, 2013, **1**, 1326.
23 C. Du, J. Zhao, J. Fei, Y. Cui and J. Li, *Adv. Healthcare Mater.*, 2013, **2**, 1246.
24 W. S. Hummers and R. E. Offeman, *J. Am. Chem. Soc.*, 1958, **80**, 1339.
25 Y.-R. V. Shih, C.-N. Chen, S.-W. Tsai, Y. J. Wang and O. K. Lee, *Stem Cells*, 2006, **24**, 2391.
26 J. Fiedler, B. Özdemir, J. Bartholomä, A. Plettl, R. E. Brenner and P. Ziemann, *Biomaterials*, 2013, **34**, 8851.
27 R. Izadpanah, C. Trygg, B. Patel, C. Kriedt, J. Dufour, J. M. Gimble and B. A. Bunnell, *J. Cell. Biochem.*, 2006, **99**, 283.
28 J. I. Paredes, S. Villar-Rodil, A. Martínez-Alonso and J. M. D. Tascón, *Langmuir*, 2008, **24**, 10560.

29 C. Shan, H. Yang, D. Han, Q. Zhang, A. Ivaska and L. Niu, *Langmuir*, 2009, **25**, 12030.
30 P. Cai, Z. Xue, W. Qi and H. Wang, *Colloids Surf., A*, 2013, **434**, 110.
31 R. Olivares-Navarrete, S. L. Hyzy, D. L. Hutton, C. P. Erdman, M. Wieland, B. D. Boyan and Z. Schwartz, *Biomaterials*, 2010, **31**, 2728.
32 T. Alava, J. A. Mann, C. Théodore, J. J. Benitez, W. R. Dichtel, J. M. Parpia and H. G. Craighead, *Anal. Chem.*, 2013, **85**, 2754.
33 F. Wang, B. Liu, A. C.-F. Ip and J. Liu, *Adv. Mater.*, 2013, **25**, 4087.
34 J. N. Tiwari, K. Mahesh, N. H. Le, K. C. Kemp, R. Timilsina, R. N. Tiwari and K. S. Kim, *Carbon*, 2013, **56**, 173.